Potential of the upcoming Biomass P-band radar mission for digital terrain modelling beneath dense tropical forests: first accuracy assessment

Mhamad El Hage [1], Ludovic Villard [2], Laurent Ferro-Famil [3,2], Laurent Polidori [4,2]

[1] Geospatial Studies Laboratory, Lebanese University, Tripoli, Lebanon;
[2] CESBIO (Centre d’Etudes Spatiales de la Biosphère), University of Toulouse, CNES/CNRS/INRAE/IRD/UPS, 31400 Toulouse, France;
[3] ISAE SUPAERO, University of Toulouse, 31400 Toulouse, France;
[4] PPGG, Institute of Geoscience, UFPA, Belém 66075-110, PA, Brazil

Keywords: Biomass, DEM, Accuracy, P-Band, SAR, Tomography, Forests

Abstract

P-band radar surveys can be used to produce digital elevation models (DEMs) at ground level in dense tropical forest areas. However, the previous performance studies were carried out on DEMs derived from high-resolution synthetic aperture radar (SAR) acquisitions, while the upcoming Biomass space mission should provide DEMs at a coarser resolution due to a frequency bandwidth of 6 MHz in range. The aim of this study is to predict the quality of the DEM products derived from Biomass data through dense forest. A DEM was produced in a slant range geometry at a 15-m mesh size using SAR tomography. It was compared to the reference LiDAR survey in terms of elevation and slope, and the statistical distribution of the corresponding error was analysed with regards to the radar off-nadir angle and to the local slope and aspect. The results show that the DEM elevation has no systematic error despite the presence of forest, and it has an RMS error of 3 meters. The DEM slope has a mean error of 2° and an RMS error of 6°. The behaviour of these errors for different terrain slopes and aspects will allow to predict the quality of Biomass DEMs on a variety of terrestrial landscapes.

1. Introduction

Digital elevation modelling through forests is a challenging task as the terrain surface is hidden below the canopy (Polidori et al., 2022). The conventional methods for producing DEM (digital elevation model) have different limitations in this regard; in optical remote sensing, the visible and infrared radiations do not penetrate the foliage. In the microwave domain, the most widely used bands (i.e., X- and C-bands) have short wavelengths which partially penetrate the canopy but do not reach the terrain. The L-band can in some circumstances reach the ground surface but in the case of high-density forests, like in the case of tropical forests, it exhibits many outliers. The only two techniques that work in this case are based on LiDAR and P-band surveys. In the case of LiDAR, part of the laser impulses reaches the ground surface, allowing a very accurate topography reconstruction by selecting and interpolating the lowest points, but this requires slow and low-height flight, which is not compatible with large-area surveys. The P-band can fully penetrate the canopy and be reflected of the terrain having some parts being reflected of the canopy (Aghababaei et al., 2020; Ferro-Famil et al., 2016; Fu et al., 2017). The challenge here is to separate the contributions of the terrain from that of the canopy (Pardini and Papathanassiou, 2017). Different methods are used for this purpose; first, interferometry with a long baseline even with a single polarization (Guimarães Filho and Borba, 2020). Second, polarimetry can be used to separate the terrain from the canopy (Fu et al., 2016; 2017). The third and most promising method is the tomography (D’Alessandro and Tebaldini, 2019; El Hage et al., 2022). This method enables the separation of the response coming from the terrain from that coming from the canopy by using SAR images acquired at different elevations. This configuration allows the synthesis of an aperture in the elevation direction is the same way as the SAR processing in the azimuth direction, thus achieving a fine angular resolution in the elevation direction. It also allows the retrieval of the reflectivity distribution in a vertical profile and to produce tomograms which are cross-sections of the forest reflectivity (Aghababaei et al., 2020; Ferro-Famil et al., 2016; Huang et al., 2011; Tebaldini et al., 2011; Villard et al., 2016) much like the CT and PET scans in medicine.

The upcoming Biomass space mission aims at estimating the global biomass using P-band SAR tomographic and interferometric data (Le Toan et al., 2011; Quegan et al., 2019) and a secondary objective is to model the elevation through forests. As part of the TropiSAR campaign undertaken by ESA for the CALVAL of the Biomass mission, a P-band radar survey has been made over the Paracou region in French Guiana (Dubois-Fernandez et al., 2010). These data have been used to evaluate the potential of Biomass for DEM production under dense forest.

DEM quality can be considered through different criteria corresponding to different user requirements. The positional quality can be assessed using external reference data based on statistical descriptors such as the mean, standard deviation and the root mean square (RMS) of the elevation error. The shape quality can be evaluated either by using external data and by the aforementioned statistical descriptors of slope error and the measurement of the spatial autocorrelation of the elevation error and its propagation into elevation derivatives, but also with internal validation methods such as the visual control and the verification of the hydrographic consistency and more generally the conformity of land relief to a number of general rules it is supposed to respect like downward water flow, Horton’s law, Benford’s law among others (Polidori and El Hage, 2020). A preliminary study (El Hage et al., 2022) aimed at evaluating the quality of a 1-m mesh size P-band DEM obtained by SAR tomography in Paracou using some of the aforementioned quality control methods and to relate the accuracy of the DEM to landscape properties and acquisition parameters; the results showed a high quality of this DEM compared with a LiDAR DEM. These results are consistent with those obtained in the

This contribution has been peer-reviewed. The double-blind peer-review was conducted on the basis of the full paper.
https://doi.org/10.5194/isprs-annals-X-3-2024-125-2024 | © Author(s) 2024. CC BY 4.0 License.

Brazilian Amazon with a 5-m mesh size DEM obtained by P-band SAR interferometry (Caldeira et al., 2023; 2024). These recent studies illustrate the potential of P-band radar for relief mapping in forested areas at high resolution. In the case of Biomass mission, the same approach can be followed but at a coarser resolution. Indeed, due to military restrictions, Biomass will use a bandwidth of only 6 MHz, which will reduce the range resolution of the SAR images and, as a consequence, that of the DEM. This paper presents the first study addressing the expected quality of Biomass DEMs.

The next section describes the study area, the data used in the study and the validation methods. Section 3 presents the results, and Section 4 discusses them and draws the conclusions.

2. Materials and Methods

2.1 Data

2.1.1 Study area: The study site is an 8 km² area located in Paracou, French Guiana at the following coordinates 52°55’55” W and 5°16’9” N (Figure 1). The area is typical of the Guiana Shield with hilly relief, a very intricate hydrographic network, a dense rainforest representative of the Amazon biome and almost no human presence.

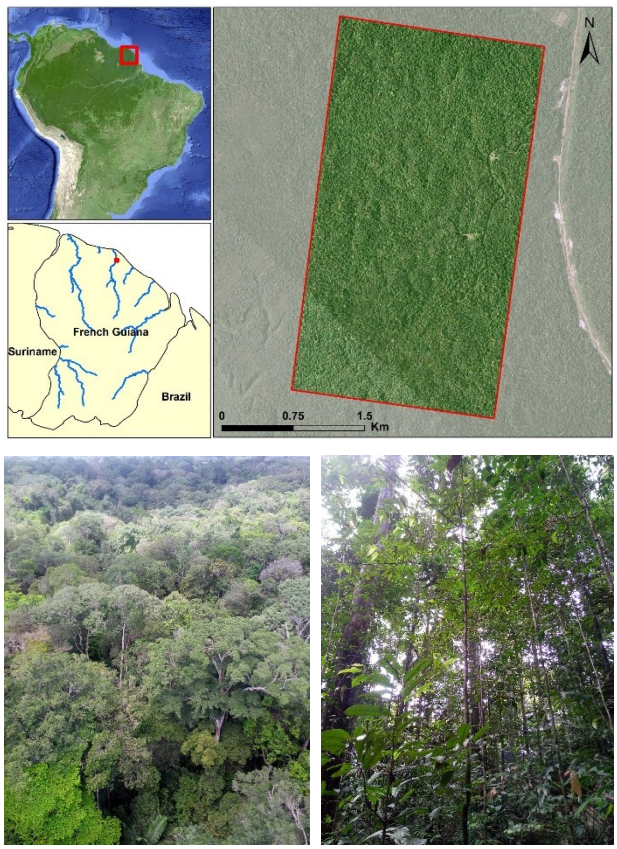

Figure 1. Location and in-situ pictures from the Guyflux tower (55m) and the so-called TropiScat plot westwards from the tower base (El Hage et al., 2022).

2.1.2 P-band DEM: The P-band DEM is produced by radar tomography using 6 fully polarimetric SAR images (Figure 2). The images were acquired in 2009 by the ONERA’s SETHI sensor (in the framework of the ESA’s TropiSAR campaign) in a repeat-pass multi-baseline InSAR mode with a carrier frequency of 397.5 MHz. The bandwidth used in the study is 6 MHz, which corresponds to that of the upcoming Biomass space mission. The spatial resolutions of the SAR images are 25 m and 12.5 m in the slant range and azimuth directions, respectively. The vertical resolution ranges between 16 m and 26 m from near to far range, respectively. The elevation angle ranges from 20° to 50°.

Tomographic imaging involves acquiring coherent radar data from slightly shifted positions to synthesize an aperture orthogonal to the radar line of sight. This process enables the synthesis of a 3D reflectivity map, with vertical resolution dependent on the length of the normalized multi-baseline aperture, the range distance and the carrier frequency (Ferro-Famil and Pottier, 2016). Polarization is utilized to further discriminate between different contributions, allowing the separation of the overall response into two components: one from the canopy and the other from the underlying ground (Tebaldini, 2009). More details on the tomographic processing are available in El Hage et al., 2022. The final DEM is resampled to a 15-m mesh size in both slant range and azimuth directions.

2.1.3 LiDAR DEM: The LiDAR DEM is generated using a helicopter mounted RIEGL LMS-280i (wavelength 0.9 µm) small-footprint LiDAR system with a ground point density of about 0.1 point/m^2 (Labrière et al., 2018). The DEM is resampled to 15-m mesh size to match that of the P-band DEM (Figure 2).

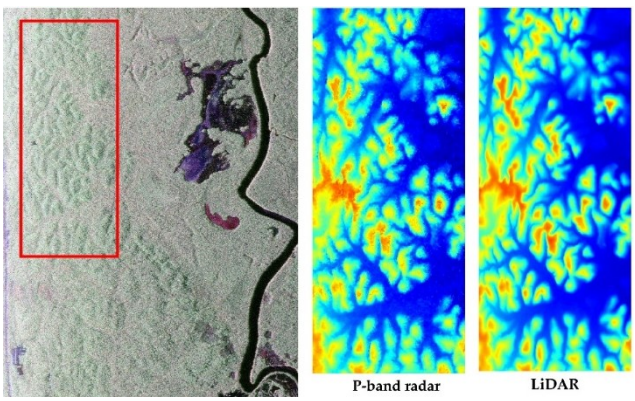

Figure 2. Subset of the original Pauli RGB image stack (left), the 1-m mesh size P-band radar tomography DEM (centre) and LiDAR DEM (right) of the area in the red frame (El Hage et al., 2022).

2.2 Methods

The error in a DEM includes three different components as shown in the following formula (Polidori and El Hage, 2020):

$$\hat{z}_i = z_i + \mu_i + \varepsilon'_i + \varepsilon''_i \quad (1)$$

where $\hat{z}_i$ is the DEM elevation, z_i is the true terrain elevation, μ_i is a systematic error, ε'_i is a random error spatially correlated and ε''_i is a spatially white noise.

The quality assessment method adopted in this study consists of external validation using ground control data. This method helps in validating the DEM positional and shape accuracies. It consists of two levels of assessment: the first one aims at characterizing the spatial distribution of the elevation difference between the DEM and the reference data using statistical descriptors such as the mean, the standard deviation and the Root Mean Square Error (RMSE), which reflect the positional accuracy but do not guarantee the shape quality (MacMillan and Shary, 2009; Temme et al., 2009).

This contribution has been peer-reviewed. The double-blind peer-review was conducted on the basis of the full paper.
https://doi.org/10.5194/isprs-annals-X-3-2024-125-2024 | © Author(s) 2024. CC BY 4.0 License.

$$\mu = \frac{1}{N}\sum_{i=1}^{N}(\hat{z}_i - z_i) \quad (2)$$

$$\sigma = \sqrt{\frac{1}{N}\sum_{i=1}^{N}(\hat{z}_i - z_i)^2 - \mu^2} \quad (3)$$

$$RMSE = \sqrt{\frac{1}{N}\sum_{i=1}^{N}(\hat{z}_i - z_i)^2} = \sqrt{\mu^2 + \sigma^2} \quad (4)$$

The second level of assessment is based on the consideration of spatial autocorrelation of the elevation errors. This autocorrelation affects, along with the elevation errors, the quality of the elevation derivatives (such as slope and curvature), which are the ultimate shape descriptors of the terrain (Heuvelink, 1998). The autocorrelation of the error is calculated using the following formula:

$$r(h) = \frac{\frac{1}{n}\sum_{i=1}^{n} d_i \times d_{i+h} - \frac{1}{n}\sum_{i=1}^{n} d_i \times \frac{1}{n}\sum_{i=1}^{n} d_{i+h}}{\sqrt{\frac{1}{n}\sum_{i=1}^{n} {d_i}^2 - \left(\frac{1}{n}\sum_{i=1}^{n} d_i\right)^2} \times \sqrt{\frac{1}{n}\sum_{i=1}^{n} {d_{i+h}}^2 - \left(\frac{1}{n}\sum_{i=1}^{n} d_{i+h}\right)^2}} \quad (5)$$

where n is the total number of point pairs, d_i and d_{i+h} are the signed differences between the two DEMs at the position i and i+h, respectively (h is the lag, i.e., distance from the position i). To assess the impact on elevation derivatives, the mean, the standard deviation and the Root Mean Square (RMS) are also calculated to characterize the slope difference between P-band and LiDAR DEMs.

Moreover, the landscape properties and acquisition parameters have an impact on the overall quality of the DEM as it was proven by many studies (El Hage, 2012). The influences of the local topography and the acquisition geometry on the quality of the P-band DEM are also investigated, mainly the effect of the terrain slope and aspect, as well as the off-nadir angle. This should provide a better understanding of the spatial distribution of the error, enabling the prediction of radar DEM errors in other regions depending on topography and acquisition parameters, and to know more about the potential of the upcoming Biomass mission for DEM production beneath dense forest.

3. Results

The statistics of the elevation and slope differences between the P-band and LiDAR DEMs are shown in Figure 3. As shown in this figure, the mean value of the elevation difference is almost null which would demonstrate that the two DEMs are very close to each other in average, confirming that P-band DEM, even at 6 MHz, has no systematic error due to the presence of forest. The mean value of slope difference is about 2° and the standard deviation is about 6°. These values are less than those obtained in (El Hage et al., 2022). This is due to the coarse resolution of the Biomass DEM which is far less than the one used in aforementioned study (1 meter), which mainly affects the elevation derivatives (El Hage et al., 2010; Santos et al., 2017). Indeed, the slope is relative and depends on the resolution of the DEM, being statistically lower at coarse resolution.

The graph of the spatial autocorrelation of elevation (Figure 4) shows high values over short distances, which is a consequence of Tobler’s first law of geography, which states that “everything is related to everything else, but near things are more related than distant things” (Miller, 2004; Tobler, 1970). The values are higher in the azimuth direction than in the range direction. Moreover, after 3 pixels, i.e., over 50 meters, the error autocorrelation becomes almost zero in the range direction. This trend does not appear in (El Hage et al., 2022), and it could primarily due to use of a 6 MHz bandwidth.

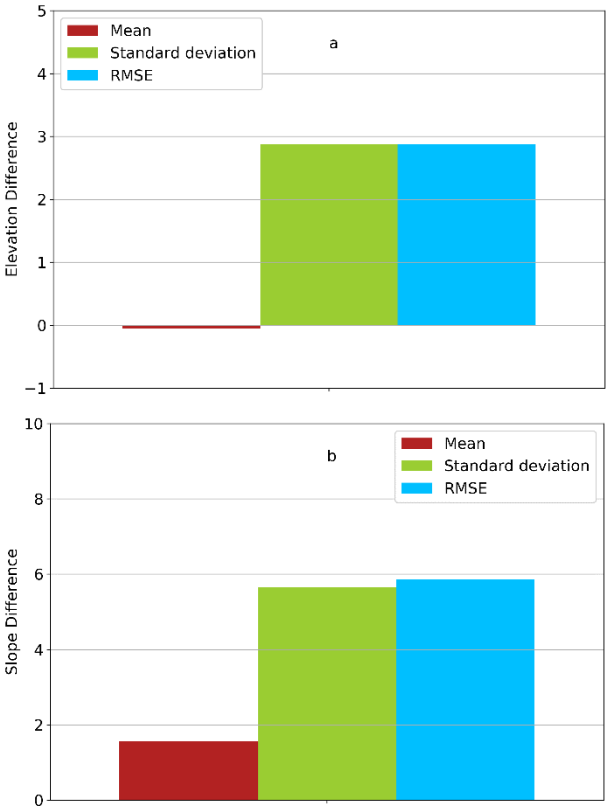

Figure 3. Elevation (m) (a) and slope (degree) (b) errors.

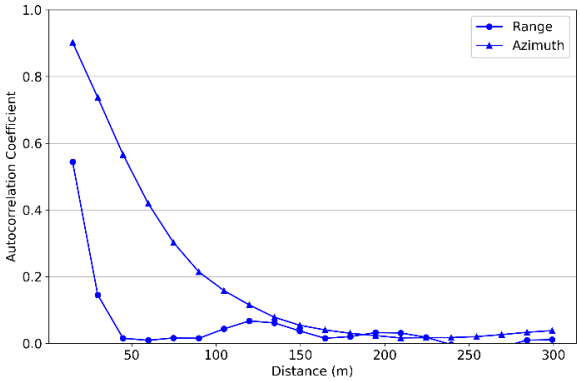

Figure 4. Spatial autocorrelation of the elevation error.

To better understand the relation between the error and the landscape and acquisition parameters, Figures 5, 6 and 7 show how the elevation and slope errors depend on the local topography (slope and aspect) and the elevation angle.

Figure 5 shows the influence of terrain slope on elevation and slope errors. There is a clear linear relationship between the mean value of elevation and slope errors and the terrain slope ($R^2 > 0.9$). The standard deviation also exhibits this linear relation specifically for the slope error. This trend is common in most theoretical studies (Oksanen and Sarjakoski, 2005) and for different techniques (El Hage et al., 2022; Papasaika and Baltsavias, 2009; Toutin, 2002). This demonstrates that the 6 MHz P-band DEM under forest exhibits the same behaviour as any other DEM in bare soil terrains.

This contribution has been peer-reviewed. The double-blind peer-review was conducted on the basis of the full paper.
https://doi.org/10.5194/isprs-annals-X-3-2024-125-2024 | © Author(s) 2024. CC BY 4.0 License.

The effect of terrain aspect is more pronounced on slope error than on the elevation error (Figure 6). The mean elevation error is almost zero and the standard deviation is around 3 m for every value of the aspect. In contrast, the standard deviation of slope error is higher in the range direction than in the azimuth direction because of the low spatial autocorrelation of the elevation error in the range direction (Figure 4).

Figure 7 shows the relation between off-nadir angle and difference of elevation and difference of slope. According to this figure, there is practically no relation between the off-nadir angle and the elevation and slope errors, with a small decrease in the slope error at high angles.

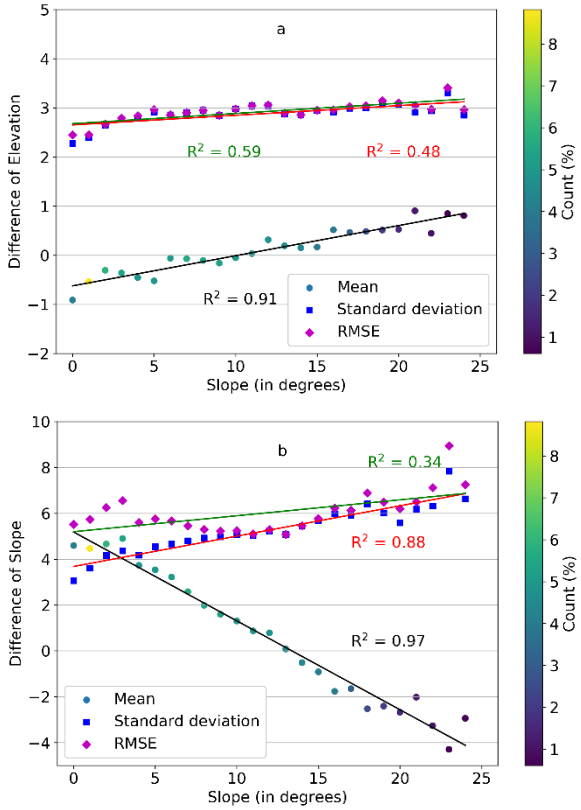

Figure 5. Statistical behaviour of elevation difference (a) and slope difference (b) as functions of terrain slope. The mean value is represented using dots, whose colour indicates the percentage of DEM points used to calculate the mean and standard deviation (see colour bar on the right side). The lines represent the regression lines for the mean, the standard deviation and the RMSE.

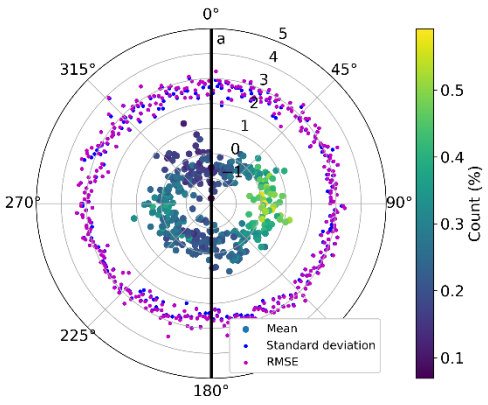

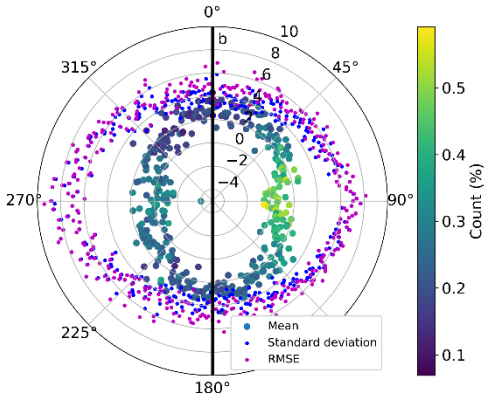

Figure 6. Influence of the slope orientation on elevation difference (a) and slope difference (b). The bold black line represents the flight direction and the illumination direction is from left to right (the right-hand half of the disks represents slopes facing away from the radar).

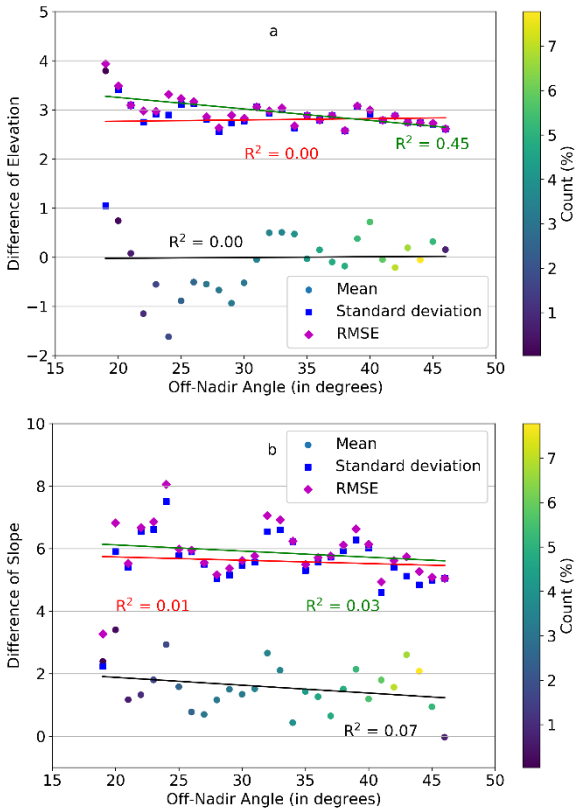

Figure 7. Statistical behaviour of elevation difference (a) and slope difference (b) as functions of the off-nadir angle. The mean value is represented using dots, whose colour indicates the percentage of DEM points used to calculate the mean and standard deviation (see colour bar on the right side). The lines represent the regression lines for the mean, the standard deviation and the RMSE.

4. Discussion and conclusions

This study presents some statistical results that give an idea of the performance to be expected from the upcoming Biomass mission for digital elevation modelling in forest regions. Following a previous study applying the same methodology to high resolution data (El Hage et al., 2022), we have now moved closer to the characteristics of Biomass in terms of resolution. It

This contribution has been peer-reviewed. The double-blind peer-review was conducted on the basis of the full paper.
https://doi.org/10.5194/isprs-annals-X-3-2024-125-2024 | © Author(s) 2024. CC BY 4.0 License.

can be seen that the degradation in resolution does not lead to a significant degradation in elevation accuracy, and that slope accuracy is even improved because of the filtering of the noise, but it also eliminates the microrelief as a consequence of a lower resolution.

One of the secondary goals of Biomass mission is to extract a quasi-global DEM, which will be distinguished from the other global DEMs such as Copernicus, SRTM, GDEM and others by the fact that it will be canopy free in forested areas that cover around 31% of the global land area in 2015 (FAO, 2015). This product should give for the first time an information on the ground elevation with a resolution comparable with nowadays available global DEMs. In airborne acquisitions, the accuracy in comparable with that of LiDAR. In spaceborne acquisitions, the advantage of P-band radar imaging over LiDAR is that it covers large areas, and, thus, it is much more suitable for cartography. These features make the upcoming Biomass DEM an invaluable source of topographic information in forested regions.

Of course, these conclusions need to be consolidated by further studies. The results presented in this paper are obtained over a small area that is a special case of a terrestrial landscape in terms of geomorphology and vegetation. Future work will apply the same methodology to other areas to confirm these initial findings and to take account of different landscapes and acquisition conditions. In addition, quality control will be extended to include different criteria, in particular those relating to the realism of landforms and the consistency of the hydrographic network. We will have to wait for the launch of the Biomass satellite and the analysis of the first data to have a definitive idea of the mission capabilities for digital terrain modelling in dense forest regions. The continental scale analysis of the Biomass tomographic data followed by several interferometric cycles (up to 5) will then offer the possibility to exploit the temporal dimension in order to improve the performances of digital terrain modelling in dense forest regions.

References

Aghababaei, H., Ferraioli, G., Ferro-Famil, L., Huang, Y., Mariotti D’Alessandro, M., Pascazio, V., Schirinzi, G., and Tebaldini, S., 2020. Forest SAR Tomography: Principles and Applications. *IEEE Geoscience and Remote Sensing Magazine*, 8, 30–45, https://doi.org/10.1109/MGRS.2019.2963093.

Caldeira, C. R. T., El Hage, M., Caldeira, M. C. O., Gorgens, E. B., Ometto, J. P. H. B., and Polidori, L., 2023. Comparison between Digital Terrain Models generated by P-Band Radar and LiDAR in the Amazon, a case study in Amapá (Brazil). *Revista de Geociências do Nordeste*, 9, 59–70, https://doi.org/10.21680/2447-3359.2023v9n1ID31573.

Caldeira, C. R. T., El Hage, M., da Silva Rosa, R. A., Polidori, L., 2024. Accuracy and hydrographic realism of an under-forest DEM derived from airborne P-band radar interferometry over a wide area in the Brazilian amazon. International Journal of Remote Sensing, 45 (16), pp. 5295 – 5316, https://doi.org/10.1080/01431161.2024.2372075.

D’Alessandro, M. M. and Tebaldini, S., 2019. Digital Terrain Model Retrieval in Tropical Forests Through P-Band SAR Tomography. *IEEE Transactions on Geoscience and Remote Sensing*, 57, 6774–6781, https://doi.org/10.1109/TGRS.2019.2908517.

Dubois-Fernandez, P., Oriot, H., Coulombeix, C., Cantalloube, H., Plessis, O. R. D., Toan, T. L., Daniel, S., Chave, J., Blanc, L., and Davidson, M., 2010. TropiSAR, a SAR data acquisition campaign in French Guiana. *8th European Conference on Synthetic Aperture Radar*, 1–4.

El Hage, M., Simonetto, E., Faour, G., and Polidori, L., 2010. Impact of DEM reconstruction parameters on topographic indices. *The International Archives of the Photogrammetry, Remote Sensing and Spatial Information Sciences*, Paris, France, 40–44.

El Hage, M., 2012. Etude de la qualité géomorphologique de modèles numériques de terrain issus de l’imagerie spatiale. *PhD Thesis*, CNAM.

El Hage, M., Villard, L., Huang, Y., Ferro-Famil, L., Koleck, T., Le Toan, T., and Polidori, L., 2022. Multicriteria Accuracy Assessment of Digital Elevation Models (DEMs) Produced by Airborne P-Band Polarimetric SAR Tomography in Tropical Rainforests. *Remote Sensing*, 14, 4173, https://doi.org/10.3390/rs14174173.

FAO: Global Forest Resources Assessment 2015. How are the world’s forests changing? *UN Food and Agriculture Organization*, Rome.

Ferro-Famil, L., Pottier, E., 2016. 2—SAR Imaging Using Coherent Modes of Diversity: SAR Polarimetry, Interferometry and Tomography, in: *Microwave Remote Sensing of Land Surface*, Baghdadi, N., Zribi, M., Eds.; Elsevier: Amsterdam, The Netherlands, pp. 67–147. ISBN 978-1-78548-159-8, https://doi.org/10.1016/B978-1-78548-159-8.50002-5.

Ferro-Famil, L., Huang, Y., and Pottier, E., 2016. Principles and Applications of Polarimetric SAR Tomography for the Characterization of Complex Environments. *VIII Hotine-Marussi Symposium on Mathematical Geodesy*, Cham, 243–255, https://doi.org/10.1007/1345_2015_12.

Fu, H., Wang, C., Zhu, J., Xie, Q., and Zhang, B., 2016. Estimation of Pine Forest Height and Underlying DEM Using Multi-Baseline P-Band PolInSAR Data. *Remote Sensing*, 8, 820, https://doi.org/10.3390/rs8100820.

Fu, H., Zhu, J., Wang, C., Wang, H., and Zhao, R., 2017. Underlying Topography Estimation over Forest Areas Using High-Resolution P-Band Single-Baseline PolInSAR Data. *Remote Sensing*, 9, 363, https://doi.org/10.3390/rs9040363.

Guimarães Filho, A. G. and Borba, P., 2020. Methodology for Land Mapping of Amapa State-A Special Case of Amazon Radiography Project. *IGARSS 2020 - 2020 IEEE International Geoscience and Remote Sensing Symposium*, 1540–1543, https://doi.org/10.1109/IGARSS39084.2020.9324673.

Heuvelink, G. B. M., 1998. Error Propagation in Environmental Modelling with GIS, Taylor and Francis, London, 156 pp., https://doi.org/10.4324/9780203016114.

Huang, Y., Ferro-Famil, L., and Lardeux, C., 2011. Polarimetric SAR tomography of tropical forests at P-Band. *IEEE International Geoscience and Remote Sensing Symposium*, 1373–1376, https://doi.org/10.1109/IGARSS.2011.6049321.

Labrière, N., Tao, S., Chave, J., Scipal, K., Toan, T. L., Abernethy, K., Alonso, A., Barbier, N., Bissiengou, P., Casal, T., Davies, S. J., Ferraz, A., Hérault, B., Jaouen, G., Jeffery, K. J., Kenfack, D., Korte, L., Lewis, S. L., Malhi, Y., Memiaghe, H. R., Poulsen, J. R., Réjou-Méchain, M., Villard, L., Vincent, G., White, L. J. T., and Saatchi, S., 2018. In Situ Reference Datasets From the TropiSAR and AfriSAR Campaigns in Support of Upcoming Spaceborne Biomass Missions, *IEEE Journal of Selected Topics in Applied Earth Observations and Remote Sensing*, 11, 3617–3627, https://doi.org/10.1109/JSTARS.2018.2851606.

Le Toan, T., Quegan, S., Davidson, M. W. J., Balzter, H., Paillou, P., Papathanassiou, K., Plummer, S., Rocca, F., Saatchi, S., Shugart, H., and Ulander, L., 2011. The BIOMASS mission: Mapping global forest biomass to better understand the terrestrial carbon cycle. *Remote Sensing of Environment*, 115, 2850–2860, https://doi.org/10.1016/j.rse.2011.03.020.

MacMillan, R. A. and Shary, P. A., 2009. Chapter 9 Landforms and Landform Elements in Geomorphometry. In: *Developments in Soil Science*, vol. 33, edited by: Hengl, T. and Reuter, H. I., Elsevier, 227–254, https://doi.org/10.1016/S0166-2481(08)00009-3.

Miller, H. J., 2004. Tobler’s First Law and Spatial Analysis. *Annals of the Association of American Geographers*, 94, 284–289, https://doi.org/10.1111/j.1467-8306.2004.09402005.x.

Oksanen, J. and Sarjakoski, T., 2005. Error propagation of DEM-based surface derivatives. *Computers & Geosciences*, 31, 1015–1027, https://doi.org/10.1016/j.cageo.2005.02.014.

Papasaika, H. and Baltsavias, E., 2009. Investigations on the Relation of Geomorphological Parameters to DEM Accuracy. *Geomorphometry Conference*, 162–168.

Pardini, M. and Papathanassiou, K., 2017. On the Estimation of Ground and Volume Polarimetric Covariances in Forest Scenarios With SAR Tomography. *IEEE Geoscience and Remote Sensing Letters*, 14, 1860–1864, https://doi.org/10.1109/LGRS.2017.2738672.

Polidori, L. and El Hage, M., 2020. Digital Elevation Model Quality Assessment Methods: A Critical Review. *Remote Sensing*, 12, 3522, https://doi.org/10.3390/rs12213522.

Polidori, L., Caldeira, C. R. T., Smessaert, M., and El Hage, M., 2022. Digital elevation modeling through forests: the challenge of the Amazon. *Acta Amaz.*, 52, 69–80, https://doi.org/10.1590/1809-4392202103091.

Quegan, S., Le Toan, T., Chave, J., Dall, J., Exbrayat, J.-F., Minh, D. H. T., Lomas, M., D’Alessandro, M. M., Paillou, P., Papathanassiou, K., Rocca, F., Saatchi, S., Scipal, K., Shugart, H., Smallman, T. L., Soja, M. J., Tebaldini, S., Ulander, L., Villard, L., and Williams, M., 2019. The European Space Agency BIOMASS mission: Measuring forest above-ground biomass from space. *Remote Sensing of Environment*, 227, 44–60, https://doi.org/10.1016/j.rse.2019.03.032.

Santos, V. C. D., El Hage, M., Polidori, L., and Stevaux, J. C., 2017. Effect of digital elevation model mesh size on geomorphic indices: a case study of the Ivaí River watershed – state of Paraná, Brazil. *Boletim de Ciências Geodésicas*, 23, 684–699, https://doi.org/10.1590/s1982-21702017000400045.

Tebaldini, S., 2009. Algebraic Synthesis of Forest Scenarios From Multibaseline PolInSAR Data. *IEEE Transactions on Geoscience and Remote Sensing*, 47, 4132–4142, https://doi.org/10.1109/TGRS.2009.2023785.

Tebaldini, S., Mariotti D’Alessandro, M., Dinh, H. T. M., and Rocca, F., 2011. P band penetration in tropical and boreal forests: Tomographical results. *IEEE International Geoscience and Remote Sensing Symposium*, 4241–4244, https://doi.org/10.1109/IGARSS.2011.6050167.

Temme, A. J. A. M., Heuvelink, G. B. M., Schoorl, J. M., and Claessens, L., 2009. Chapter 5 Geostatistical Simulation and Error Propagation in Geomorphometry, in: *Developments in Soil Science*, vol. 33, edited by: Hengl, T. and Reuter, H. I., Elsevier, 121–140, https://doi.org/10.1016/S0166-2481(08)00005-6.

Tobler, W. R., 1970. A Computer Movie Simulating Urban Growth in the Detroit Region. *Economic Geography*, 46, 234–240, https://doi.org/10.2307/143141.

Toutin, T., 2002. Impact of terrain slope and aspect on radargrammetric DEM accuracy. *ISPRS Journal of Photogrammetry and Remote Sensing*, 57, 228–240, https://doi.org/10.1016/S0924-2716(02)00123-5.

Villard, L., Le Toan, T., Ho Tong Minh, D., Mermoz, S., and Bouvet, A., 2016. 9 - Forest Biomass From Radar Remote Sensing. In: *Land Surface Remote Sensing in Agriculture and Forest*, edited by: Baghdadi, N. and Zribi, M., Elsevier, 363–425, https://doi.org/10.1016/B978-1-78548-103-1.50009-1.